Supporting Information for: Chemical Potentials of Water, Methanol, Carbon Dioxide, and Hydrogen Sulfide at Low Temperatures using Continuous Fractional Component Gibbs Ensemble Monte Carlo

Ahmadreza Rahbari,[†] Ali Poursaeidesfahani,[†] Ariana Torres-Knoop,[‡] David Dubbeldam,[‡] and Thijs J.H. Vlugt[*,†]

†*Engineering Thermodynamics, Process & Energy Department, Faculty of Mechanical, Maritime and Materials Engineering, Delft University of Technology, Leeghwaterstraat 39, 2628CB, Delft, The Netherlands*

‡*Van't Hoff Institute for Molecular Sciences, University of Amsterdam, Science Park 904, 1098XH Amsterdam, The Netherlands*

E-mail: t.j.h.vlugt@tudelft.nl

In the Overlapping Distribution Method[1] (ODM), two systems are considered with equal volume V: *(1)*: system 0 with N particles; *(2)*: system 1 with $N+1$ particles. This method constructs a histogram of the interaction potential of a test particle in system 0 ($p_0(\Delta U)$), and a histogram of the interaction potential of a randomly selected molecule in system 1 ($p_1(\Delta U)$). Constructing these histograms per number of formed hydrogen bonds between the test particle and its surrounding particles leads to the formulation of a two-dimensional ODM. The canonical partition function of system 0 equals

$$Q_0\left(N,V,T\right)=\frac{V^N}{\Lambda^{3N}N!}q_0 \tag{S1}$$

V is the volume, and Λ is the de Broglie thermal wavelength. q_0 is the configurational part of the partition function of system 0

$$q_0=\int \mathrm{d}s^N \exp\left[-\beta U_0\left(s^N\right)\right] \tag{S2}$$

U_0 denotes the total potential energy of system 0, and s^N are the reduced coordinates of the particles in the system. The logarithm of probability of finding an interaction potential energy change ΔU in a trial insertion when the test particle forms H_T hydrogen bonds (integer) with its surrounding particles can be written in the canonical ensemble

$$\ln p_0\left(\Delta U,H_{\mathrm{T}}\right)=\ln\left[\frac{\int \mathrm{d}s^N \exp\left[-\beta U_0\right]\delta\left(U_i-\Delta U\right)\delta\left(H_i-H_{\mathrm{T}}\right)}{q_0}\right] \tag{S3}$$

U_i is the interaction potential energy of the test particle in system 0 with the rest of the particles. H_i is the number of formed hydrogen bonds between the test particle and its surrounding molecules. For system 1, the canonical partition function of a system with $N+1$ molecules equals

$$Q_1\left(N+1,V,T\right)=\frac{V^{N+1}}{\Lambda^{3N+3}(N+1)!}q_1 \tag{S4}$$

q_1 is the configurational part of the partition function of system 1

$$q_1=\int \mathrm{d}s^{N+1} \exp\left[-\beta U_1\left(s^{N+1}\right)\right] \tag{S5}$$

U_1 is the total potential energy of system 1.

The logarithm of probability of finding an interaction potential energy change ΔU in a trial removal when the particle has H_T hydrogen bonds with its surrounding molecules, can be written in the canonical ensemble

$$\ln p_1\left(\Delta U, H_{\mathrm{T}}\right)=\ln\left[\frac{\int \mathrm{d}s^{N+1}\exp\left[-\beta U_1\right]\delta\left(U_r-\Delta U\right)\delta\left(H_r-H_{\mathrm{T}}\right)}{q_1}\right] \tag{S6}$$

U_r is the interaction potential energy of a random particle in system 1 in a trial removal move. H_r is the number of formed hydrogen bonds between this particle and its surrounding particles in system 1. Combining Eqs. S4 and S6 leads to

$$\ln p_1\left(\Delta U, H_{\mathrm{T}}\right)=\ln\left[\frac{V^{N+1}}{\Lambda^{3N+3}\left(N+1\right)!Q\left(N+1,V,T\right)}\left(\begin{array}{l}\int \mathrm{d}s^{N}\exp\left[-\beta U_0\right]\int \mathrm{d}s\exp\left[-\beta\Delta U\right]\\ \times\,\delta\left(U_r-\Delta U\right)\delta\left(H_r-H_{\mathrm{T}}\right)\end{array}\right)\right] \tag{S7}$$

One can write

$$\frac{V^{N+1}}{\Lambda^{3N+3}\left(N+1\right)!Q_1\left(N+1,V,T\right)}=\frac{V^{N}}{\Lambda^{3N}N_1}\cdot\frac{V/\Lambda^3}{N+1}\cdot\frac{1}{Q_1\left(N+1,V,T\right)} \tag{S8}$$

Combining Eqs. S1 and S8 leads to

$$\frac{V/\Lambda^3}{N+1}\cdot\frac{1}{Q_1\left(N+1,V,T\right)}\cdot\frac{V^{N}}{\Lambda^{3N}N_1}\cdot\frac{q_0}{q_0}=\frac{V/\Lambda^3}{N+1}\cdot\frac{Q_0\left(N,V,T\right)}{Q_1\left(N+1,V,T\right)}\cdot\frac{1}{q_0} \tag{S9}$$

Rearraning equation Eq. S7 based on Eq. S9

$$\ln p_1\left(\Delta U, H_{\mathrm{T}}\right)=\ln\left[\frac{V^N/\Lambda^3\,Q_0\left(N,V,T\right)}{\left(N+1\right)Q_1\left(N+1,V,T\right)}\cdot\frac{1}{q_0}\cdot\left(\begin{array}{l}\int \mathrm{d}s^{N}\exp\left[-\beta U_0\right]\times\\ \delta\left(U_r-\Delta U\right)\delta\left(H_r-H_{\mathrm{T}}\right)\end{array}\right)\right]-\beta\Delta U \tag{S10}$$

Combining Eqs. S3 and S10 leads to

$$\begin{aligned}\ln p_1\left(\Delta U, H_{\mathrm{T}}\right)&=\ln\left(\frac{V^N/\Lambda^3\,Q_0\left(N,V,T\right)}{\left(N+1\right)Q_1\left(N+1,V,T\right)}\cdot p_0\left(\Delta U, H_{\mathrm{T}}\right)\right)-\beta\Delta U\\&=\ln\left(\frac{Q_0\left(N,V,T\right)}{Q_1\left(N+1,V,T\right)}\right)+\ln\left(\frac{V/\Lambda^3}{N+1}\right)+\ln p_0\left(\Delta U, H_{\mathrm{T}}\right)-\beta\Delta U\end{aligned} \tag{S11}$$

The chemical potential equals[2]

$$\mu = -k_B T \ln\left(\frac{Q(N+1,V,T)}{Q(N,V,T)}\right) \tag{S12}$$

The ideal part of the chemical potential is defined as

$$\mu^{\mathrm{id}} = -k_B T \ln\left(\frac{V/\Lambda^3}{N+1}\right) \tag{S13}$$

Combining Eqs. S11 to S13 leads to

$$\begin{aligned} \ln p_1\left(\Delta U, H_{\mathrm{T}}\right) &= \beta\mu - \beta\mu^{\mathrm{id}} + \ln p_0\left(\Delta U, H_{\mathrm{T}}\right) - \beta\Delta U \\ &= \beta\mu^{\mathrm{ex}} + \ln p_0\left(\Delta U, H_{\mathrm{T}}\right) - \beta\Delta U \end{aligned} \tag{S14}$$

Rearranging equation Eq. S14, leads to

$$\left[\frac{1}{\beta}\left(\ln p_1\left(\Delta U, H_{\mathrm{T}}\right)\right) + \frac{\Delta U}{2}\right] - \left[\frac{1}{\beta}\left(\ln p_0\left(\Delta U, H_{\mathrm{T}}\right)\right) - \frac{\Delta U}{2}\right] = \mu^{\mathrm{ex}} \tag{S15}$$

The functions in the brackets are labeled $f_1\left(\Delta U, H_{\mathrm{T}}\right)$ and $f_0\left(\Delta U, H_{\mathrm{T}}\right)$ respectively. The excess chemical potential is therefore obtained by subtracting these two functions

$$f_1\left(\Delta U, H_{\mathrm{T}}\right) - f_0\left(\Delta U, H_{\mathrm{T}}\right) = \mu^{\mathrm{ex}} \tag{S16}$$

Based on Rosenbluth sampling method,[3] Mooij and Frankel[4–6] have shown that in case of successive insertion or removal of chain molecules, or orientational biasing, $-\beta\Delta U$ in Eq. S16 should be replaced by logarithm of W. Then, functions f_0 and f_1 equal

$$f_0\left(W, H\right) = \frac{1}{\beta}\left[\ln p_0\left(\ln W\right) + \frac{\ln W}{2}\right] \tag{S17}$$

$$f_1\left(W, H\right) = \frac{1}{\beta}\left[\ln p_1\left(\ln W\right) - \frac{\ln W}{2}\right] \tag{S18}$$

Table S1: Vapor-Liquid coexistence densities and chemical potentials of OPLS-UA methanol[7] obtained from Gibbs Ensemble Monte Carlo simulations. Chemical potentials computed with the Widom's Test Particle Insertion (WTPI) method are denoted by μ^{WTPI}. Chemical potentials directly computed using CFCMC GE simulations[8] are denoted by μ^{CFCMC}. Chemical potentials at phase equilibrium obtained by an empirical equation of state for methanol[9] using REFPROP[10] are denoted by μ^{EOS}. The subscripts g and l refer to the gas and liquid phases respectively. Numbers in brackets are uncertainties in the last digit, i.e., -31(1) means -31 $\pm$ 1. The error bars in the CFCMC method are much smaller compared to the WTPI method. Temperatures, densities and chemical potentials are reported in units of [K], [kg.m^{-3}] and [kJ.mol^{-1}], respectively.

T	ρ_l^{CFCMC}	ρ_g^{CFCMC}	ρ_l^{GE}	ρ_g^{GE}	μ_l^{CFCMC}	μ_g^{CFCMC}	μ_l^{WTPI}	μ_g^{WTPI}	μ^{EOS}
250	805(1)	0.019(1)	806(2)	0.018(1)	-30.7(1)	-31.2(2)	-23(1)	-30.9(1)	-34.84
290	766(3)	0.178(7)	767(1)	0.182(6)	-30.1(1)	-30.5(1)	-24(1)	-30.41(8)	-30.63
320	738(1)	0.85(4)	734(2)	0.75(4)	-29.4(1)	-29.6(1)	-26(2)	-29.8(1)	-30.50
350	702(2)	2.6(2)	705(2)	2.7(1)	-29.3(3)	-29.4(2)	-26(1)	-29.2(1)	-30.05
375	672(2)	6.1(1)	627(2)	5.9(1)	-29.2(1)	-29.16(6)	-27(1)	-29.2(2)	-29.96

Table S2: Vapor-Liquid coexistence densities and chemical potentials of TraPPE methanol[11] obtained from Gibbs Ensemble Monte Carlo simulations. Chemical potentials computed with the Widom's Test Particle Insertion (WTPI) method are denoted by μ^{WTPI}. Chemical potentials directly computed using CFCMC GE simulations[8] are denoted by μ^{CFCMC}. Chemical potentials at phase equilibrium obtained by an empirical equation of state for methanol[9] using REFPROP[10] are denoted by μ^{EOS}. The subscripts g and l refer to the gas and liquid phases respectively. Numbers in brackets are uncertainties in the last digit, i.e., -30.9(8) means -30.9 $\pm$ 0.8. The error bars in the CFCMC method are much smaller compared to the WTPI method. Temperatures, densities and chemical potentials are reported in units of [K], [kg.m^{-3}] and [kJ.mol^{-1}], respectively.

T	ρ_l^{CFCMC}	ρ_g^{CFCMC}	ρ_l^{GE}	ρ_g^{GE}	μ_l^{CFCMC}	μ_g^{CFCMC}	μ_l^{WTPI}	μ_g^{WTPI}	μ^{EOS}
250	825(1)	0.0136(3)	831.0(4)	0.0127(7)	-31.7(1)	-31.9(1)	-24(1)	-30.6(1)	-34.84
290	797(2)	0.41(1)	792(2)	0.127(6)	-30.0(3)	-29.9(3)	-25(1)	-31.2(1)	-30.63
320	758(1)	0.54(3)	759(2)	0.51(2)	-30.9(2)	-30.8(1)	-26(1)	-30.9(2)	-30.50
350	726(1)	1.9(1)	728(3)	1.9(2)	-30.6(1)	-30.38(6)	-27(1)	-30.3(6)	-30.05
375	695(2)	4.2(1)	697(1)	4.3(2)	-30.5(1)	-30.24(7)	-27(1)	-30.1(1)	-29.96

Table S3: Vapor-Liquid coexistence densities and chemical potentials of TraPPE carbon dioxide[12] obtained from Gibbs Ensemble Monte Carlo simulations. Chemical potentials computed with the WTPI method are denoted by μ^{WTPI}. Chemical potentials directly computed using CFCMC GE simulations[8] are denoted by μ^{CFCMC}. Chemical potentials at phase equilibrium obtained by an empirical equation of state for carbon dioxide[13] using REFPROP[10] are denoted by μ^{EOS}. Chemical potentials directly computed using CFCMC GE simulations are denoted by μ^{CFCMC}. The subscripts g and l refer to the gas and liquid phases respectively. Numbers in brackets are uncertainties in the last digit, i.e., -16.3(1) means -16.3 $\pm$ 0.1. The error bars in the CFCMC method are much smaller compared to the WTPI method. Temperatures, densities and chemical potentials are reported in units of [K], [kg.m^{-3}] and [kJ.mol^{-1}], respectively.

T	ρ_l^{CFCMC}	ρ_g^{CFCMC}	ρ_l^{GE}	ρ_g^{GE}	μ_l^{CFCMC}	μ_g^{CFCMC}	μ_l^{WTPI}	μ_g^{WTPI}	μ^{EOS}
220	1156(1)	14.7(6)	1159(1)	15.0(2)	-15.50(8)	-15.83(7)	-15.83(4)	-15.81(2)	-14.80
230	1121(2)	21.8(7)	1122(2)	22.1(5)	-15.57(3)	-15.89(4)	-15.90(6)	-15.88(3)	-14.95
240	1082(1)	31.6(6)	1084(2)	31.8(6)	-15.66(4)	-15.96(3)	-15.97(5)	-15.97(3)	-15.13
250	1042(1)	44(1)	1043(1)	44.6(9)	-15.80(5)	-16.07(7)	-16.08(3)	-16.08(3)	-15.33

Table S4: Vapor-Liquid coexistence densities and chemical potentials of hydrogen sulfide[14] obtained from Gibbs Ensemble Monte Carlo simulations. Chemical potentials computed with WTPI method are denoted by μ^{WTPI}. Chemical potentials directly computed using CFCMC GE simulations are denoted by μ^{CFCMC}. Chemical potentials at phase equilibrium obtained by an empirical equation of state for hydrogen sulfide[15] using REFPROP[10] are denoted by μ^{EOS}.The subscripts g and l refer to the gas and liquid phases respectively. Numbers in brackets are uncertainties in the last digit, i.e., 1.8(2) means 1.8 ± 0.2. Temperatures, densities and chemical potentials are reported in units of [K], [kg.m^{-3}] and [kJ.mol^{-1}], respectively.

T	ρ_l^{CFCMC}	ρ_g^{CFCMC}	ρ_l^{GE}	ρ_g^{GE}	μ_l^{CFCMC}	μ_g^{CFCMC}	μ_l^{WTPI}	μ_g^{WTPI}	μ^{EOS}
210	950(2)	1.8(2)	950(1)	1.82(5)	-17.4(1)	-18.0(2)	-17.9(2)	-18.12(4)	-18.16
220	932(2)	3.0(1)	932(1)	2.8(1)	-17.4(1)	-18.1(1)	-18.1(1)	-18.20(8)	-18.22
230	913(3)	4.3(3)	914.8(3)	4.41(8)	-17.7(1)	-18.3(2)	-18.1(1)	-18.24(4)	-18.30
240	897(1)	6.3(4)	896.2(6)	6.3(1)	-17.7(1)	-18.3(2)	-18.34(8)	-18.35(3)	-18.41
250	878(2)	8.9(6)	877.9(1)	8.8(1)	-17.87(5)	-18.4(1)	-18.51(5)	-18.49(3)	-18.52

Table S5: Vapor-Liquid coexistence densities and chemical potentials of SPC,[16,17] TIP3P-EW,[18] TIP4P-EW[19] and TIP5P-EW[20] water obtained from Gibbs Ensemble Monte Carlo simulations. Chemical potentials computed with the Widom's test particle insertion method are denoted by μ^{WTPI}. Chemical potentials directly computed using CFCMC GE simulations are denoted by μ^{CFCMC}. Chemical potentials at phase equilibrium obtained by the IAPWS empirical equation of state for water[21] using REFPROP[10] are denoted by μ^{EOS}. The subscripts g and l refer to the gas and liquid phases respectively. Numbers in brackets are uncertainties in the last digit, i.e., -36.6(5) means -36.6 ± 0.5. The chemical potentials in the liquid and gas phases obtained from CFCMC GE simulations are almost equal within the error bars. Temperatures, densities and chemical potentials are reported in units of [K], [kg.m^{-3}] and [kJ.mol^{-1}], respectively.

T	ρ_l^{CFCMC}	ρ_g^{CFCMC}	ρ_l^{GE}	ρ_g^{GE}	μ_l^{CFCMC}	μ_g^{CFCMC}	μ_l^{WTPI}	μ_g^{WTPI}	μ^{EOS}
SPC									
300	977(1)	0.029(1)	976(1)	0.029(1)	-33.9(3)	-34.49(8)	-30(1)	-34.51(1)	-34.84
325	957(1)	0.104(3)	955(1)	0.104(2)	-33.5(3)	-34.03(9)	-30(1)	-34.0(1)	-34.34
350	932(1)	0.303(7)	932(1)	0.303(4)	-33.2(3)	-33.63(8)	-31(1)	-33.62(7)	-33.93
TIP3P-EW									
300	993.4(6)	0.028(1)	996(1)	0.029(6)	-34.2(3)	-34.6(1)	-29(1)	-34.5(1)	-34.84
325	972(1)	0.101(3)	974(1)	0.108(1)	-33.8(4)	-34.1(1)	-30(1)	-33.9(1)	-34.34
350	946.8(4)	0.320(8)	946(1)	0.309(2)	-33.3(3)	-33.5(1)	-31(1)	-33.63(6)	-33.93
TIP4P-EW									
300	991(3)	0.0079(8)	994(1)	0.0008(2)	-36.6(5)	-37.2(2)	-30(2)	-37.41(4)	-34.84
325	980(2)	0.034(2)	980(1)	0.033(1)	-36.0(2)	-36.8(2)	-31.3(8)	-37.07(6)	-34.34
350	963(1)	0.112(4)	966(1)	0.108(2)	-35.6(3)	-36.4(1)	-32.0(9)	-36.53(8)	-33.93
TIP5P-EW									
300	999(3)	0.063(7)	997(1)	0.0650(3)	-31.9(5)	-32.6(2)	-27(1)	-32.5(2)	-34.84
325	982(2)	0.214(8)	979(1)	0.210(1)	-31.4(4)	-32.0(1)	-28(3)	-32.1(1)	-34.84
350	958(1)	0.60(2)	953.0(7)	0.620(3)	-31.0(5)	-31.58(3)	-29.1(9)	-31.5(1)	-33.93

Table S6: Force field parameters for SPC,[16,17] TIP3P-EW,[18] TIP4P-EW,[19] and TIP5P-EW.[20] SPC water is a rigid model with bond length O–H=1Å and a bond angle of H–O–H=109.47°. TIP3P-EW water and TIP4P-EW are rigid as well, both with bond length of O-H=0.9572Å and a rigid bend of H-O-H=104.52°. The dummy site of the TIP4P-EW model is located on the bisector of H-O-H angle with a distance of 0.125AA from the oxygen atom. TIP5P-EW is also with a bond length of O–H=0.9572Å and a rigid bend of H–O–H=104.52°, this model has two dummy sites M1 and M2 with a distance of 0.7Å from the oxygen atom, with the angle M1-O-M2=109.47°. The Ewald summation was used for Coulombic interactions with a relative precision of 10^{-6}.[22,23]

Atom type	ϵ/k_B/[K]	σ/[Å]	q/[e]
SPC			
O	78.2	3.166	-0.82
H	0.0	0.0	0.41
TIP3P-EW			
O	51.3287	3.188	-0.83
H	0.0	0.0	0.415
TIP4P-EW			
O	81.8994	3.16435	0.0
H	0.0	0.0	0.52422
M	0.0	0	-1.04844
TIP5P-EW			
O	89.633	3.097	0
H	0.0	0.0	0.241
M1	0.0	0.0	-0.241
M2	0.0	0.0	-0.241

Table S7: Force field parameters and model descriptions of methanol,[9] hydrogen sulfide[15] and carbon dioxide.[13] OPLS-UA methanol has rigid bonds between oxygen, hydrogen and the carbon group (O–H=0.945, C–O=1.43), and a rigid bend (C–O–H=108.5°). Intermolecular interactions are of OPLS-UA Methanol are truncated and at 12Å with tail corrections. TraPPE methanol has a flexible structure with a flexible bend (CH_3-O-H=108.5° and k_θ/k_B=55400, [K/rad^2], and constant bond length between oxygen, hydrogen and the carbon group (CH_3-O=1.43Å, O-H=0.945Å). A spherical cutoff of 14Å and tail corrections are used for this model. hydrogen sulfide has a bond length S–H=1.4Å and a dummy site (M) located at a distance of 0.1863Å on the bisector of the H-S-H angle. Intermolecular interactions of hydrogen sulfide are truncated at 14Å with analytical tail corrections. The TraPPE carbon dioxide is a rigid model (C–O=1.16). The Ewald summation was used for Coulombic interactions with a relative precision of 10^{-6}.[22,23]

Atom type	ϵ/k_B/[K]	σ/[Å]	q/[e]
Methanol OPLS-UA			
CH_3	104.165	3.775	0.265
O	85.5468	3.07	-0.7
H	0.0	0.0	0.435
Methanol TraPPE			
CH_3	98.0	3.75	0.265
O	93.0	3.02	-0.7
H	0.0	0.0	0.435
Hydrogen Sulfide			
S	250	3.73	0.40
M	0.0	0.0	-0.90
H	0.0	0.0	0.25
Carbon dioxide TraPPE			
C	27.0	2.8	0.7
O	79.0	3.05	-0.35

Table S8: Molecular volume of water, methane hydrogen sulfide and carbon dioxide molecule. The volume of each Lennard-Jones interaction site with diameter σ equals: $V = \frac{4}{3}\pi(\sigma/2)^3$. The volume of each molecule equals the sum of all the LJ interaction sites minus the overlapping volume between the interaction sites.

Molecule	Water	Methane	Hydrogen sulfide	Carbon dioxide
Volume/[Å^3]	16.60	34.98	27.17	31.0122

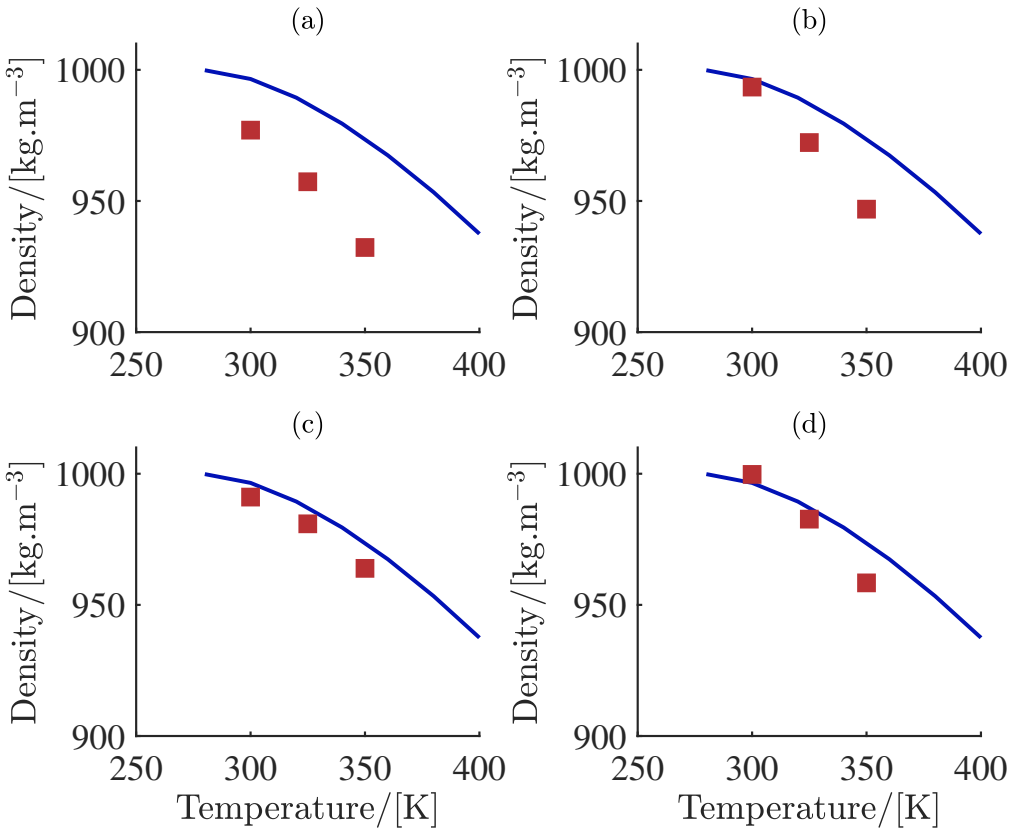

Figure S1: Liquid densities of water using different models (a) ■: SPC,[16,17] (b) ■: TIP3P-EW,[18] (c) ■: TIP4P-EW,[19] (d) ■: TIP5P-EW[20] based on vapor-liquid equilibria from GE simulations between $T = 300$K to $T = 350$K, compared to empirical equation of state.[10] In all subplots: (—): IAPWS equation of state[21] provided by NIST, REFPROP.[10] Error bars are smaller than symbol sizes.

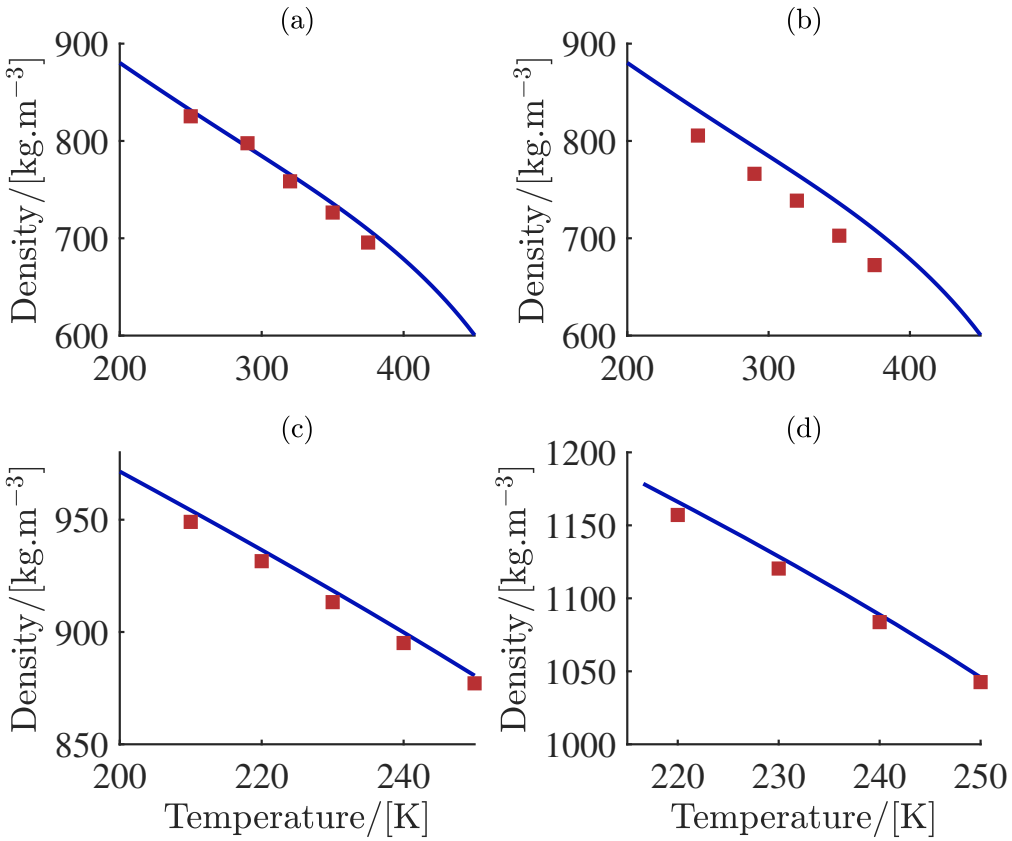

Figure S2: Saturated liquid densities of methanol, hydrogen sulfide and carbon dioxide obtained based on vapor-liquid equilibria from GE simulations between $T = 220$K to $T = 360$K, compared to an empirical equation of state provided by NIST, REFPROP.[10] In all subplots: (a) ▫: flexible methanol TraPPE model,[11] (—): empirical equation of state; (b) ▫: rigid methanol OPLS-UA model,[7] (—): empirical equation of state; (c) ▫: hydrogen sulfide,[14] (—): empirical equation of state; (d) ▫: carbon dioxide TraPPE model,[12] (—): empirical equation of state.

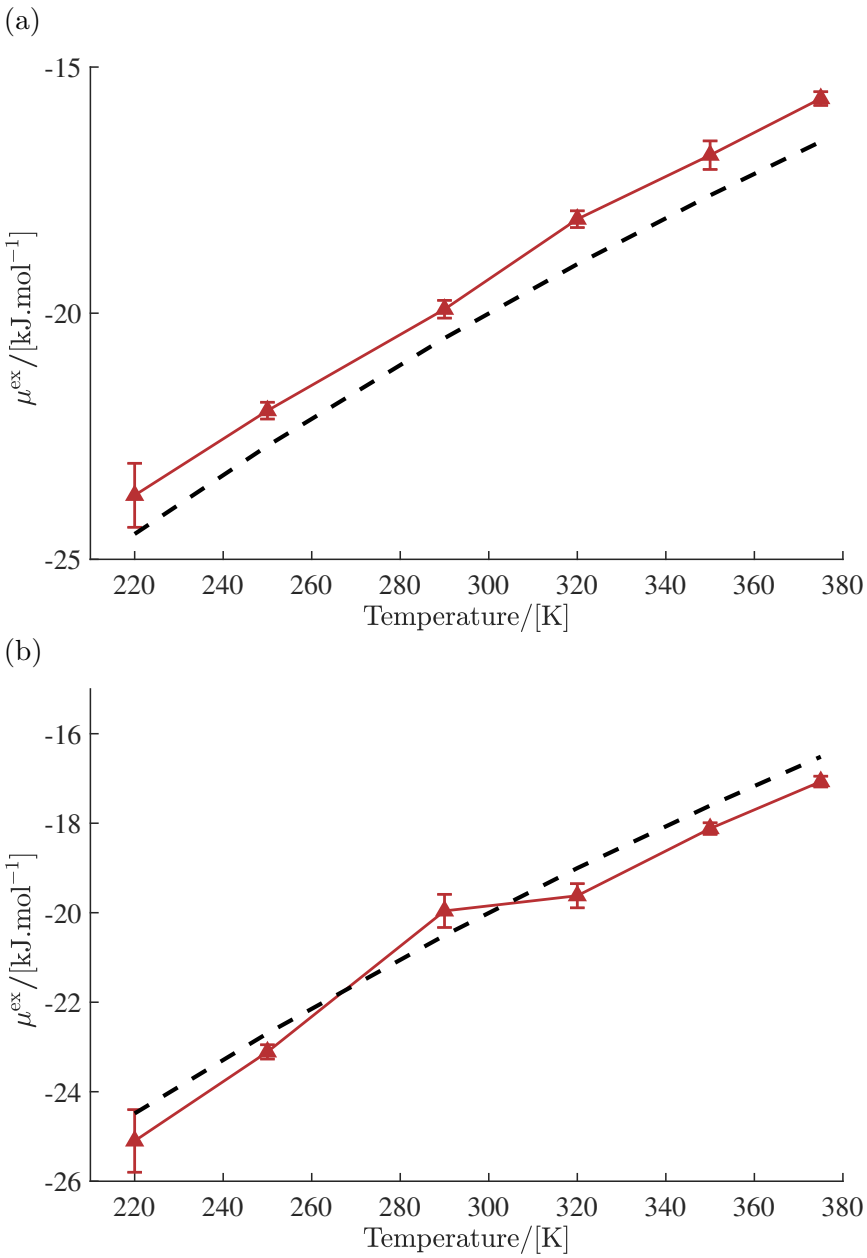

Figure S3: Computed excess chemical potentials of methanol at the vapor-liquid coexistence line with the CFCGE MC method and comparison with empirical data: (a) ▲: OPLS-UA methanol model, (– – –): Helmholtz equation of state[9] based on empirical data of methanol, provided by NIST, REFPROP[10] (b) ▲: TraPPE methanol model, (– – –): Helmholtz equation of state.

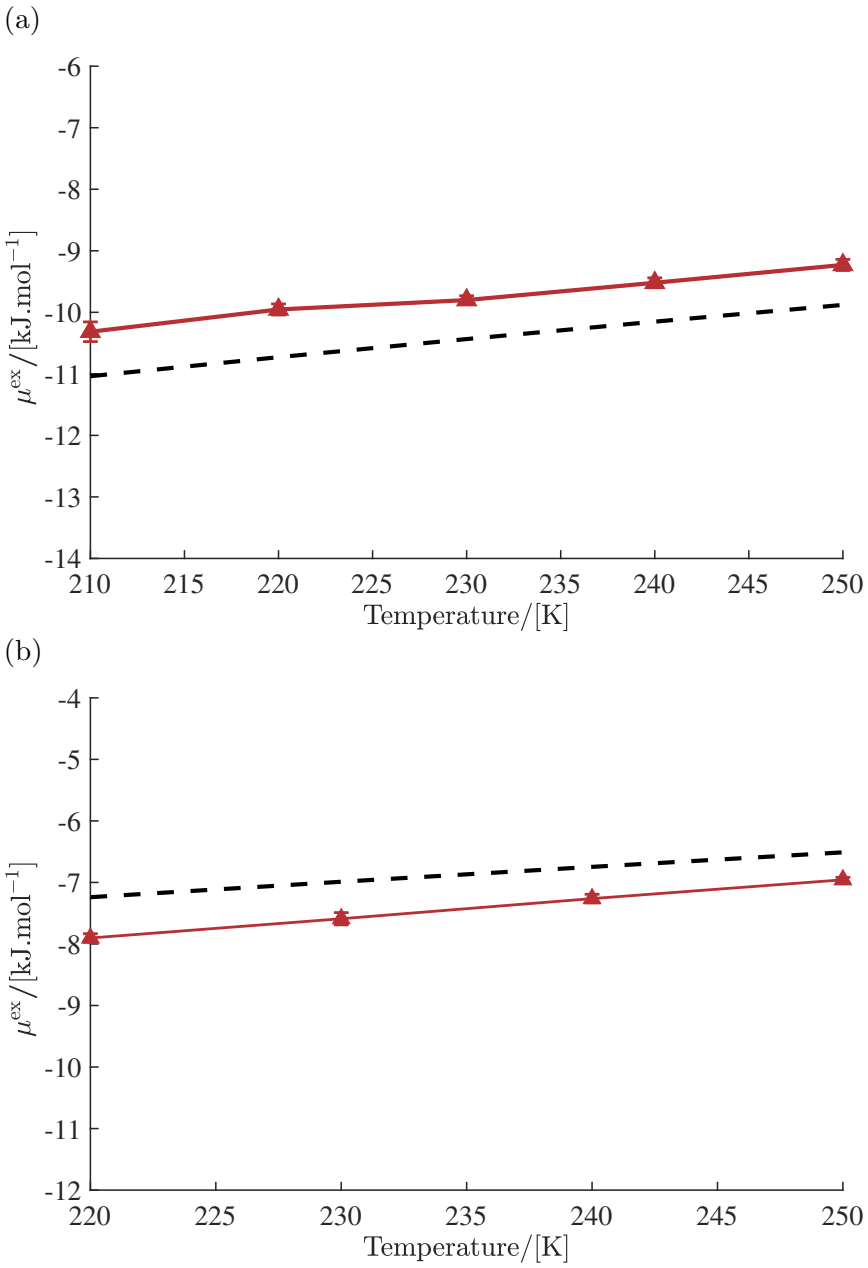

Figure S4: Computed excess chemical potentials of hydrogen sulfide and carbon dioxide at the vapor-liquid coexistence line with CFCGE MC method and comparison with empirical data: (a) ▲: hydrogen sulfide model, (– – –): Helmholtz equation of state[15] and (b) ▲: TraPPE carbon dioxide model, (– – –): Helmholtz equation of state,[13] provided by NIST, REFPROP.

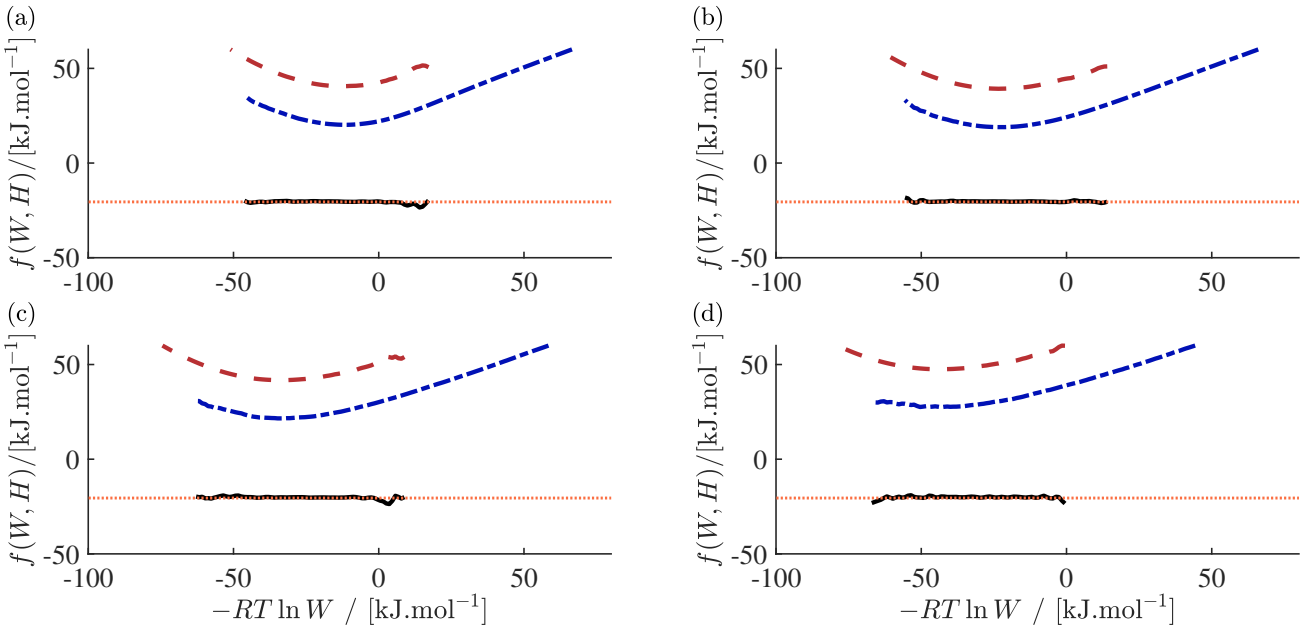

Figure S5: Two-dimensional overlapping distribution method applied to the TIP4P-EW liquid water model in the NVT ensemble at T=500K and void a fraction of $\phi = 0.55$. The sampled hydrogen bond count in each subplot equals: (a) $H = 0$; (b) $H = 1$; (c) $H = 2$; (d) $H = 3$. In all subplots: (– – –): $f_1(W,H)$, (– · –): $f_0(W,H)$, (···): $\mu^{\mathrm{ex}}_{\mathrm{WTPI}}$, (——): $f_0(W,H) - f_1(W,H)$.

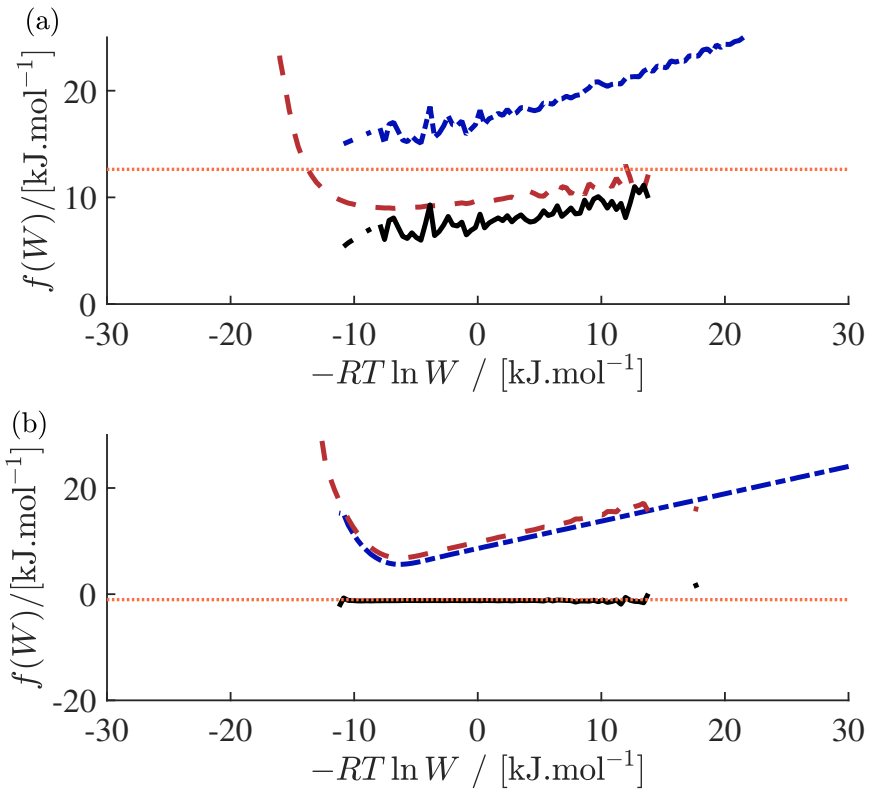

Figure S6: Overlapping distribution method applied to the Lennard-Jones liquid in the NVT ensemble at reduced temperature $T^* = 1.2$ and different reduced densities: (a) $\rho^* = 1.1$, $\phi = 0.42$; (b) $\rho^* = 0.7$, $\phi = 0.63$. In all subplots: (– – –): $f_1(W)$, (–·–): $f_0(W)$, (···): $\mu^{\mathrm{ex}}_{\mathrm{WTPI}}$, (——): $f_0(W) - f_1(W)$. Reduced temperatures and densities are defined as: $T^* = k_B T/\epsilon$, $\rho^* = \rho\sigma^3$.

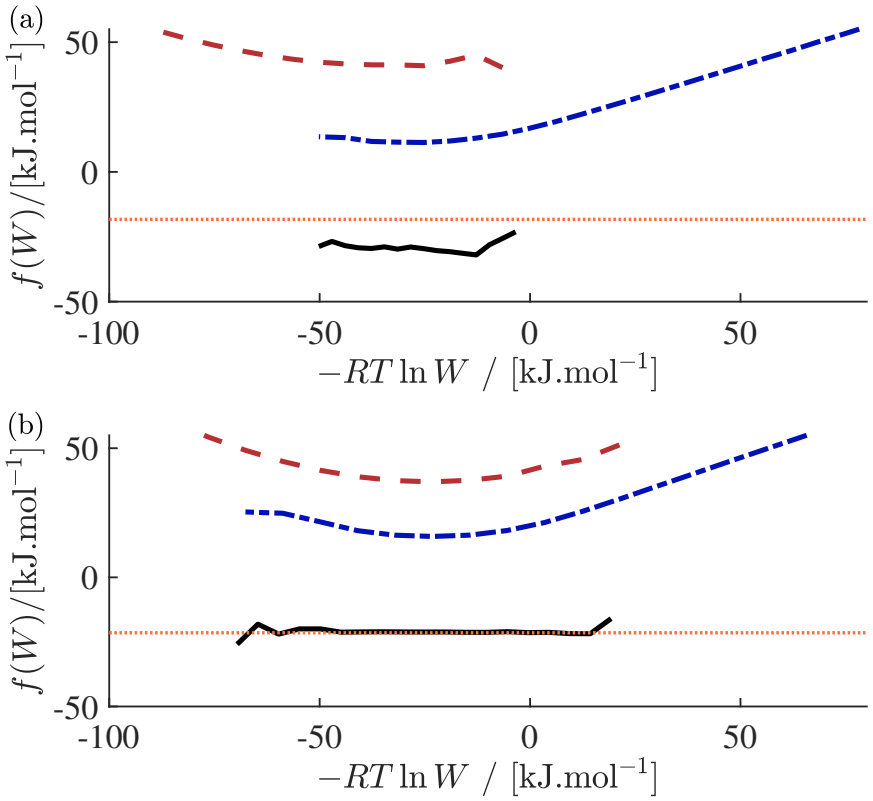

Figure S7: Overlapping distribution method compared to the WTPI results in the NVT ensemble for liquid water (TIP4P-EW), based on the coexistence densities computed from the GE simulations for four different void fractions: (a) T=300K, $\phi = 0.45$; (b) T=475K, $\phi = 0.53$. In all subplots: (– – –): $f_1(W)$, (–·–): $f_0(W)$, (···): $\mu^{\mathrm{ex}}_{\mathrm{WTPI}}$, (——): $f_0(W) - f_1(W)$

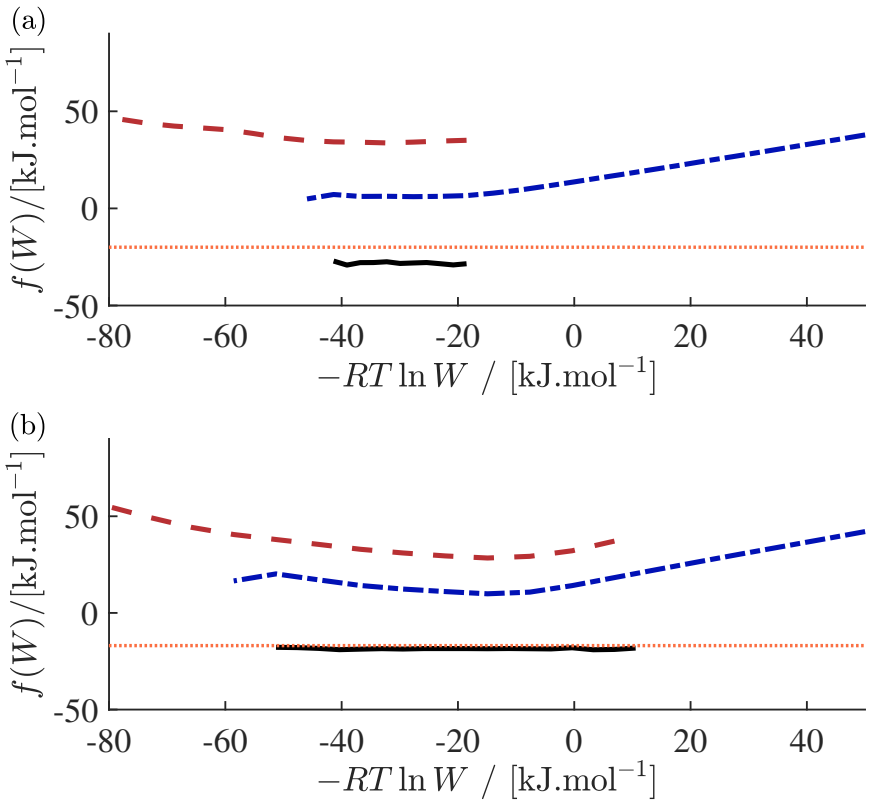

Figure S8: Overlapping distribution method compared to the WTPI results in the NVT ensemble for liquid methanol (OPLS-UA), based on the coexistence densities computed from the GE simulations for four different void fractions: (a) T=220K, $\phi = 0.45$; (b) T=350K, $\phi = 0.55$. In all subplots: (– – –): $f_1(W)$, (–·–): $f_0(W)$, (···): $\mu^{\mathrm{ex}}_{\mathrm{WTPI}}$, (——): $f_0(W) - f_1(W)$

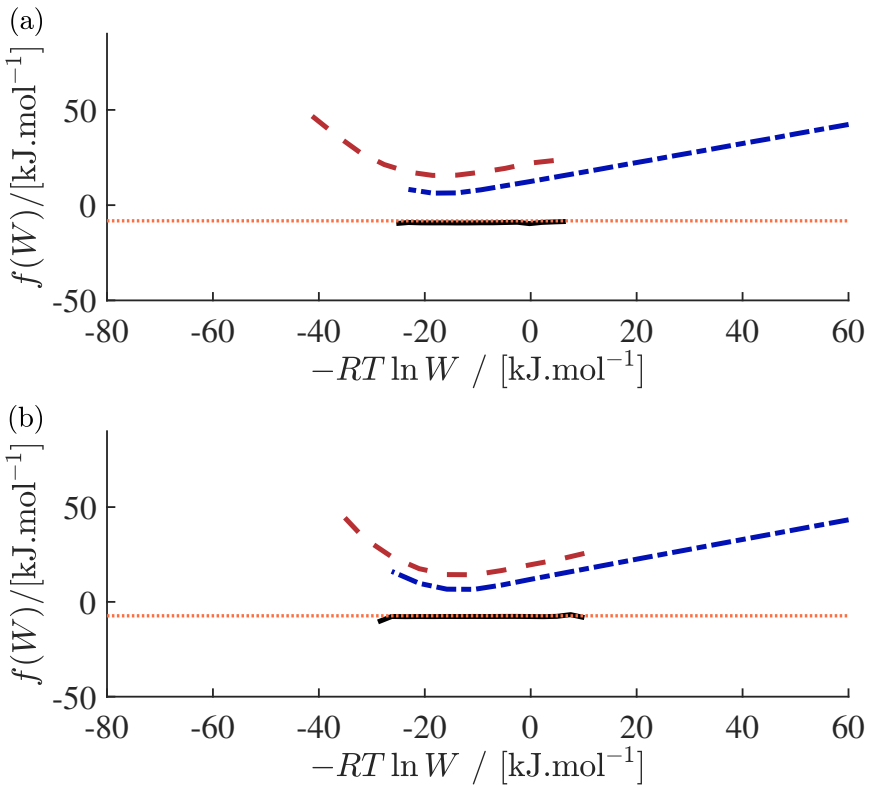

Figure S9: Overlapping distribution method compared to the WTPI results in the NVT ensemble for liquid carbon dioxide, based on the coexistence densities computed from the GE simulations for four different void fractions: (a) T=220K, $\phi = 0.51$; (b) T=250K, $\phi = 0.56$. In all subplots: (– – –): $f_1(W)$, (–·–): $f_0(W)$, (···): $\mu^{\mathrm{ex}}_{\mathrm{WTPI}}$, (——): $f_0(W) - f_1(W)$

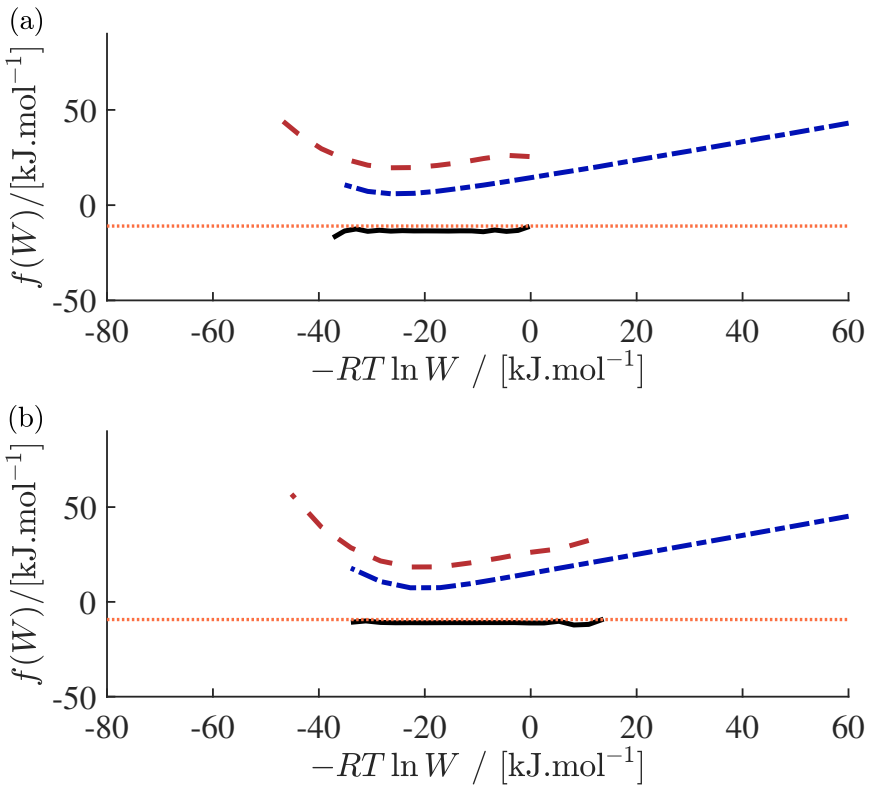

Figure S10: Overlapping distribution method compared to the WTPI results in the NVT ensemble for liquid hydrogen sulfide, based on the coexistence densities computed from the GE simulations for four different void fractions: (a) T=210K, $\phi = 0.54$; (b) T=270K, $\phi = 0.60$. In all subplots: (– – –): $f_1(W)$, (–·–): $f_0(W)$, (···): $\mu^{\mathrm{ex}}_{\mathrm{WTPI}}$, (——): $f_0(W) - f_1(W)$

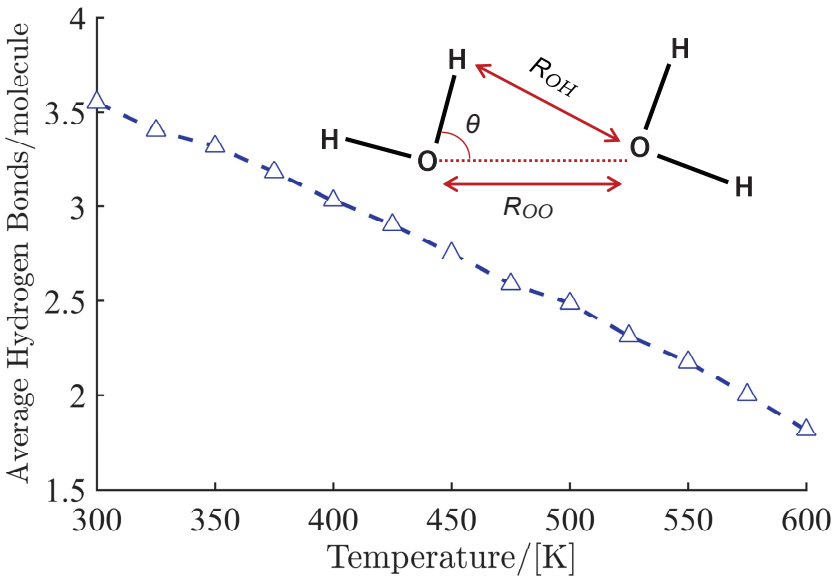

Figure S11: Hydrogen bond geometric criterion[24–29] between two water molecules: $R_{\mathrm{OO}} < 3.5$ Å, $R_{\mathrm{OH}} < 2.5$ Å and $\theta < 30$. △: Average number of hydrogen bonds for the TIP4P-EW water model computed in the NVT ensemble based on the coexistence densities of saturated liquid water from NIST database.[10]

References

(1) Mooij, G. C. A. M.; Frenkel, D. The overlapping distribution method to compute chemical potentials of chain molecules. *J. Phys.: Condens. Matt.* **1994**, *6*, 3879–3888.

(2) Smit, B.; Frenkel, D. Calculation of the chemical potential in the Gibbs ensemble. *Mol. Phys.* **1989**, *68*, 951–958.

(3) Rosenbluth, M. N.; Rosenbluth, A. W. Monte Carlo calculation of the average extension of molecular chains. *J. Comput. Phys.* **1955**, *23*, 356–359.

(4) Mooij, G. C. A. M.; Frenkel, D. The overlapping distribution method to compute chemical potentials of chain molecules. *J. Phys.: Condens. Matt.* **1994**, *6*, 3879–3888.

(5) Frenkel, D.; Smit, B. *Understanding molecular simulation: from algorithms to applications*, 2nd ed.; Academic Press: San Diego, California, 2002.

(6) Willemsen, S.; Vlugt, T.; Hoefsloot, H.; Smit, B. Combining dissipative particle dynamics and Monte Carlo techniques. *J. Comput. Phys.* **1998**, *147*, 507–517.

(7) Jorgensen, W. L. Optimized intermolecular potential functions for liquid alcohols. *J. Phys. Chem.* **1986**, *90*, 1276–1284.

(8) Poursaeidesfahani, A.; Torres-Knoop, A.; Dubbeldam, D.; Vlugt, T. J. H. Direct Free Energy Calculation in the Continuous Fractional Component Gibbs Ensemble. *J. Chem. Theory Comput.* **2016**, *12*, 1481–1490.

(9) De Reuck, K.; Craven, R. Methanol, international thermodynamic tables of the fluid state, vol. 12. *IUPAC, Blackwell Scientific Publications, London* **1993**,

(10) Lemmon, E. W.; Huber, M. L.; McLinden, M. O. NIST reference fluid thermodynamic and transport properties–REFPROP. *NIST SRData* **2013**, v9.1.

(11) Chen, B.; Potoff, J. J.; ; Siepmann, J. I. Monte Carlo calculations for alcohols and their mixtures with alkanes. Transferable potentials for phase equilibria. 5. United-atom description of primary, secondary and tertiary alcohols. *J. Phys. Chem. B* **2001**, *105*, 3093–3104.

(12) Potoff, J. J.; Siepmann, J. I. Vapor–liquid equilibria of mixtures containing alkanes, carbon dioxide, and nitrogen. *AIChE J.* **2001**, *47*, 1676–1682.

(13) Span, R.; Wagner, W. A new equation of state for carbon dioxide covering the fluid region from the triple-point temperature to 1100 K at pressures up to 800 MPa. *J. Phys.: Chem. Ref. Data.* **1996**, *25*, 1509–1596.

(14) Shah, M. S.; Tsapatsis, M.; Siepmann, J. I. Development of the Transferable Potentials for Phase Equilibria Model for Hydrogen Sulfide. *J. Phys. Chem. B* **2015**, *119*, 7041–7052.

(15) Lemmon, E. W.; Span, R. Short fundamental equations of state for 20 industrial fluids. *J. Chem. Eng. Data* **2006**, *51*, 785–850.

(16) Pullman, A. *Intermolecular forces*, 1st ed.; Springer Science & Business Media: Dordrecht, Holland, 2013; Vol. 14.

(17) Jorgensen, W. L.; Chandrasekhar, J.; Madura, J. D.; Impey, R. W.; Klein, M. L. Comparison of simple potential functions for simulating liquid water. *J. Comput. Phys.* **1983**, *79*, 926–935.

(18) Price, D. J.; Brooks III, C. L. A modified TIP3P water potential for simulation with Ewald summation. *J. Comput. Phys.* **2004**, *121*, 10096–10103.

(19) Horn, H. W.; Swope, W. C.; Pitera, J. W.; Madura, J. D.; Dick, T. J.; Hura, G. L.; Head-Gordon, T. Development of an improved four-site water model for biomolecular simulations: TIP4P-Ew. *J. Comput. Phys.* **2004**, *120*, 9665–9678.

(20) Rick, S. W. A reoptimization of the five-site water potential (TIP5P) for use with Ewald sums. *J. Comput. Phys.* **2004**, *120*, 6085–6093.

(21) Wagner, W.; Pruß, A. The IAPWS formulation 1995 for the thermodynamic properties of ordinary water substance for general and scientific use. *J. Phys.: Chem. Ref. Data.* **2002**, *31*, 387–535.

(22) Dubbeldam, D.; Calero, S.; Ellis, D. E.; Snurr, R. Q. RASPA: molecular simulation software for adsorption and diffusion in flexible nanoporous materials. *Mol. Sim.* **2016**, *42*, 81–101.

(23) Dubbeldam, D.; Torres-Knoop, A.; Walton, K. S. On the inner workings of Monte Carlo codes. *Mol. Sim.* **2013**, *39*, 1253–1292.

(24) Ferrario, M.; Haughney, M.; McDonald, I. R.; Klein, M. L. Moleculardynamics simulation of aqueous mixtures: Methanol, acetone, and ammonia. *J. Comput. Phys.* **1990**, *93*, 5156–5166.

(25) Luzar, A.; Chandler, D. Structure and hydrogen bond dynamics of waterdimethyl sulfoxide mixtures by computer simulations. *J. Comput. Phys.* **1993**, *98*, 8160–8173.

(26) Luzar, A.; Chandler, D. Hydrogen-bond kinetics in liquid water. *Nature* **1996**, *379*, 55.

(27) Jedlovszky, P.; Brodholt, J.; Bruni, F.; Ricci, M.; Soper, A.; Vallauri, R. Analysis of the hydrogen-bonded structure of water from ambient to supercritical conditions. *J. Comput. Phys.* **1998**, *108*, 8528–8540.

(28) Luzar, A. Resolving the hydrogen bond dynamics conundrum. *J. Comput. Phys.* **2000**, *113*, 10663–10675.

(29) Bauer, B. A.; Patel, S. Properties of water along the liquid-vapor coexistence curve via molecular dynamics simulations using the polarizable TIP4P-QDP-LJ water model. *J. Comput. Phys.* **2009**, *131*, 084709.